



Australian Journal of Earth Sciences

An International Geoscience Journal of the Geological Society of Australia

ISSN: (Print) (Online) Journal homepage: <https://www.tandfonline.com/loi/taje20>

Tectonic setting and mineralisation potential of the Cowley Ophiolite Complex, north Queensland

A. Edgar, I. V. Sanislav & P. H. G. M. Dirks

To cite this article: A. Edgar, I. V. Sanislav & P. H. G. M. Dirks (2022): Tectonic setting and mineralisation potential of the Cowley Ophiolite Complex, north Queensland, Australian Journal of Earth Sciences, DOI: [10.1080/08120099.2022.2086173](https://doi.org/10.1080/08120099.2022.2086173)

To link to this article: <https://doi.org/10.1080/08120099.2022.2086173>



© 2022 The Author(s). Published by Informa UK Limited, trading as Taylor & Francis Group.



[View supplementary material](#)



Published online: 27 Jun 2022.



[Submit your article to this journal](#)



[View related articles](#)



[View Crossmark data](#)

Tectonic setting and mineralisation potential of the Cowley Ophiolite Complex, north Queensland

A. Edgar , I. V. Sanislav  and P. H. G. M. Dirks 

Economic Geology Research Centre, College of Science and Engineering, James Cook University, Townsville, Australia

ABSTRACT

Northeast Queensland contains multiple slices of mafic–ultramafic units, strung out along regional faults that mark major tectonic boundaries. One such complex is the Cowley Ophiolite Complex, which is situated along the Russell–Mulgrave Fault. The Cowley Ophiolite Complex is a differentiated mafic–ultramafic complex composed of gabbro, chlorite schist, anthophyllite schist and serpentinite. We interpret that the alteration assemblages observed throughout the Cowley Ophiolite Complex reflect an amphibolite facies metasomatic overprint within a supra-subduction zone setting. This interpretation is consistent with geochemical discrimination of the gabbro, and chromite grains from the anthophyllite schist. The Cowley Ophiolite Complex records a higher metamorphic grade than the surrounding Hodgkinson Formation, and we interpret this to reflect the allochthonous structural setting of the complex, positioned along an ancient subduction margin. This subduction margin is represented today by the Russell–Mulgrave Fault. Metasomatism and emplacement of the complex probably pre-dated deposition of the Mossman Orogen’s active margin successions. Our interpretation of an active subduction complex, which pre-dated the formation of the Mossman Orogen, suggests that the Russell–Mulgrave Fault is a Paleozoic, continental suture zone. The Cowley Ophiolite Complex presents little indication of economic mineralisation; however, much of the complex remains unexplored.

KEY POINTS

1. The Cowley Ophiolite Complex is a differentiated, mafic–ultramafic complex formed within a supra-subduction zone setting.
2. Emplacement of the Cowley Ophiolite Complex, along the Russell–Mulgrave Fault, pre-dated the formation of the Hodgkinson Province.
3. The Russell–Mulgrave Fault represents an ancient subduction margin, and is interpreted as a Paleozoic, continental suture zone.

ARTICLE HISTORY

Received 13 March 2022
Accepted 26 May 2022

KEYWORDS

geology; tectonics; geochemistry; Tasmanides; ophiolite; mineral potential; critical metals

Introduction

Laterite-hosted ore deposits that form on top of mafic–ultramafic complexes have the potential to host significant resources of critical metals such as Ni, Cr, Co and Sc. Laterite deposits contribute over 60% of the global Ni supply (Butt & Cluzel, 2013). Major resources include the Weda Bay deposit in Indonesia (117 Mt @ 1.3 wt% Ni; Farrokhpay *et al.*, 2019) and the Koniambo deposit in New Caledonia (158.6 Mt @ 2.47 wt% Ni; Cathelineau *et al.*, 2016). Ni laterite deposits formed as a result of pervasive weathering of mafic–ultramafic bedrock by meteoric fluids, generally in high precipitation environments. Metals, such as Ni, Cr, Co and Sc, were mobilised from primary silicates, and

redistributed and concentrated into the overlying stratigraphy (Gleeson *et al.*, 2003). Ni laterite deposits have been identified in rocks that formed from the Archean to the Paleozoic across various tectonic settings including accretionary environments, stable cratons and rift settings (Gleeson *et al.*, 2003; Maier *et al.*, 2008). Favourable bedrock lithologies include komatiites, layered ultramafic intrusive complexes and ophiolite complexes (Elias, 2002).

Ophiolite complexes have the potential to host substantial, lateritic, Ni–Cr–Co mineralisation, and their occurrence may provide clues about the regional tectonic history (Butt & Cluzel, 2013; Lewis *et al.*, 2006). Ophiolite complexes comprise mafic–ultramafic slices of oceanic lithosphere that

CONTACT Alexander Edgar  alexander.edgar@my.jcu.edu.au  Economic Geology Research Centre, College of Science and Engineering, James Cook University, Townsville, 4811, Australia
Editorial handling: Chris Fergusson

 Supplemental data for this article is available online at <https://doi.org/10.1080/08120099.2022.2086173>

© 2022 The Author(s). Published by Informa UK Limited, trading as Taylor & Francis Group.

This is an Open Access article distributed under the terms of the Creative Commons Attribution-NonCommercial-NoDerivatives License (<http://creativecommons.org/licenses/by-nc-nd/4.0/>), which permits non-commercial re-use, distribution, and reproduction in any medium, provided the original work is properly cited, and is not altered, transformed, or built upon in any way.

were tectonically emplaced onto continental crust during orogenesis (Furnes & Dilek, 2017; Pearce, 2014; Yilmaz & Yilmaz, 2013). Ophiolite complexes are mostly interpreted to have formed along active plate margins. They were traditionally interpreted as sequences of MORB-like oceanic crust that were emplaced along subduction zones during obduction processes atop of an overriding plate. However, most preserved ophiolite complexes have been re-interpreted as being formed within a supra-subduction zone setting (Dilek & Furnes, 2014; Shervais, 2001). Ophiolite complexes are commonly associated with arc–continent or continent–continent collisional terrains (Dilek & Furnes, 2011), although they have also been recognised within backarc basins that experienced extension and subsequent subduction initiation and/or thrusting during basin closure (Božović *et al.*, 2013; Wang *et al.*, 2002). However, ophiolite complexes generated within backarc environments are rarely preserved, owing to the eventual subduction of the backarc and ophiolite sequences during basin closure (Draut & Clift, 2013).

The rocks exposed in northeast Queensland contain several mafic–ultramafic complexes positioned along major structural terrain boundaries. One such boundary is the tectonised contact between the Proterozoic Georgetown Inlier with the Paleozoic Greenvale Province along the Lynd Mylonite Zone (Fergusson *et al.*, 2007). Within the Greenvale Province, Ni laterites have developed above ultramafic complexes (Arnold & Rubenach, 1976), including the ‘Sconi’ lateritic Ni–Co–Cr–Sc deposits, which comprise >75 Mt of ore at 0.6 wt% Ni and 0.08 wt% Co (Australian Mines ASX Announcement, 29 April 2019). These ultramafic complexes were initially interpreted as layered ultramafic intrusions by Arnold and Rubenach (1976), but they acknowledged the possibility of an ophiolite origin.

Numerous occurrences of ultramafic rocks have been documented along the coastal, north–northwest–striking Russell–Mulgrave Fault. The most significant of these is the Cowley Ophiolite Complex (COC), a 4 × 1 km north–northwest–striking complex, situated 20 km south of Innisfail. The genesis of the COC is unknown, and its mineral potential has been poorly constrained despite similarities to the host rocks to the Greenvale Ni–Co–Cr–Sc deposits inland. In this contribution, we investigate the genesis and mineralisation potential of the COC and discuss the implications of the ophiolite complexes for the tectonic evolution of northeast Queensland.

Geological setting

The rocks in northeast Queensland record a prolonged geological history that starts with the Paleo- and Mesoproterozoic rocks of the Georgetown (Boger & Hansen, 2004; Murgulov *et al.*, 2007), Coen (Blewett & Black, 1998) and Yambo inliers through to the Neoproterozoic–Paleozoic rocks of the Tasmanides (Glen, 2005; Rosenbaum, 2018; Withnall & Henderson, 2012). Bound to the west by the Tasman Line, the Tasmanides comprise five major orogenic belts across eastern Australia.

The Tasmanides have been interpreted to record evidence for long-lived, accretionary-style tectonic events, in which continent growth occurred without the addition of exotic terrains and collisional tectonics (Cawood *et al.*, 2009). Popular tectonic models (Collins, 2002; Glen, 2013; Gray & Foster, 2004) describe accordion-style switching between extensional and compressional tectonic periods, facilitated by the gradual eastward retreat of a westward-dipping subduction complex. Periods of extension, attributed to slab rollback, were associated with widespread backarc basin development, magmatism and sedimentation. Slab break-off, slab flattening and jamming of the outboard subduction margin are thought to have triggered sporadic shifts to compressional tectonics. Periods of orogeny were relatively short-lived and marked by widespread basin inversion of arc and backarc assemblages. Shortening was generally east–west and accompanied by metamorphic conditions up to amphibolite facies.

Aitchison and Buckman (2012) suggested an alternative to the single, long-lived subduction complex model. Their model, which they termed ‘quantum tectonics’, infers that numerous subduction complexes were active throughout the Paleozoic. They argued that polarity reversals of these subduction zones facilitated the accretion of oceanic arcs that contributed significantly to the growth of eastern Australia. A study by Dirks *et al.* (2021) has provided further evidence for collisional tectonics within the Tasmanides following the identification of accreted oceanic crust along the Paleo-Pacific convergent margin.

The Tasmanides in northeast Queensland comprise the exposed margin of the Thomson Orogen, and the Mossman Orogen. The Thomson Orogen comprises the Charters Towers Province and Greenvale Province. Henderson *et al.* (2020) described the Charters Towers Province as consisting of Neoproterozoic, meta-sedimentary and meta-igneous basement rocks that were overlain by an early Paleozoic backarc succession, which formed in response to the westward retreat of a Paleo-Pacific subduction complex. Lateral exposure of the Charters Towers Province is restricted to the south by younger cover sequences. The province was emplaced to the north against the younger Broken River Province along the Clarke River Fault. This margin was interpreted as a convergent margin (Figure 1; Dirks *et al.*, 2021). The Greenvale Province represents the northwestern most extension of the Thomson Orogen. To the north, the Greenvale Province is in contact with the Paleo to Mesoproterozoic Georgetown Inlier along the Lynd Mylonite Zone (Fergusson *et al.*, 2007). To the east, the Greenvale Province was faulted against the Broken River Province along the Greenvale Fault. The Greenvale Province contains a sequence of lower Paleozoic, meta-sediments and meta-igneous basement rocks that are overlain by basin infill deposited in a backarc setting (Fergusson *et al.*, 2007; Withnall & Henderson, 2012).

The Mossman Orogen is situated to the north–northeast of the Thomson Orogen, and it represents the northern-most

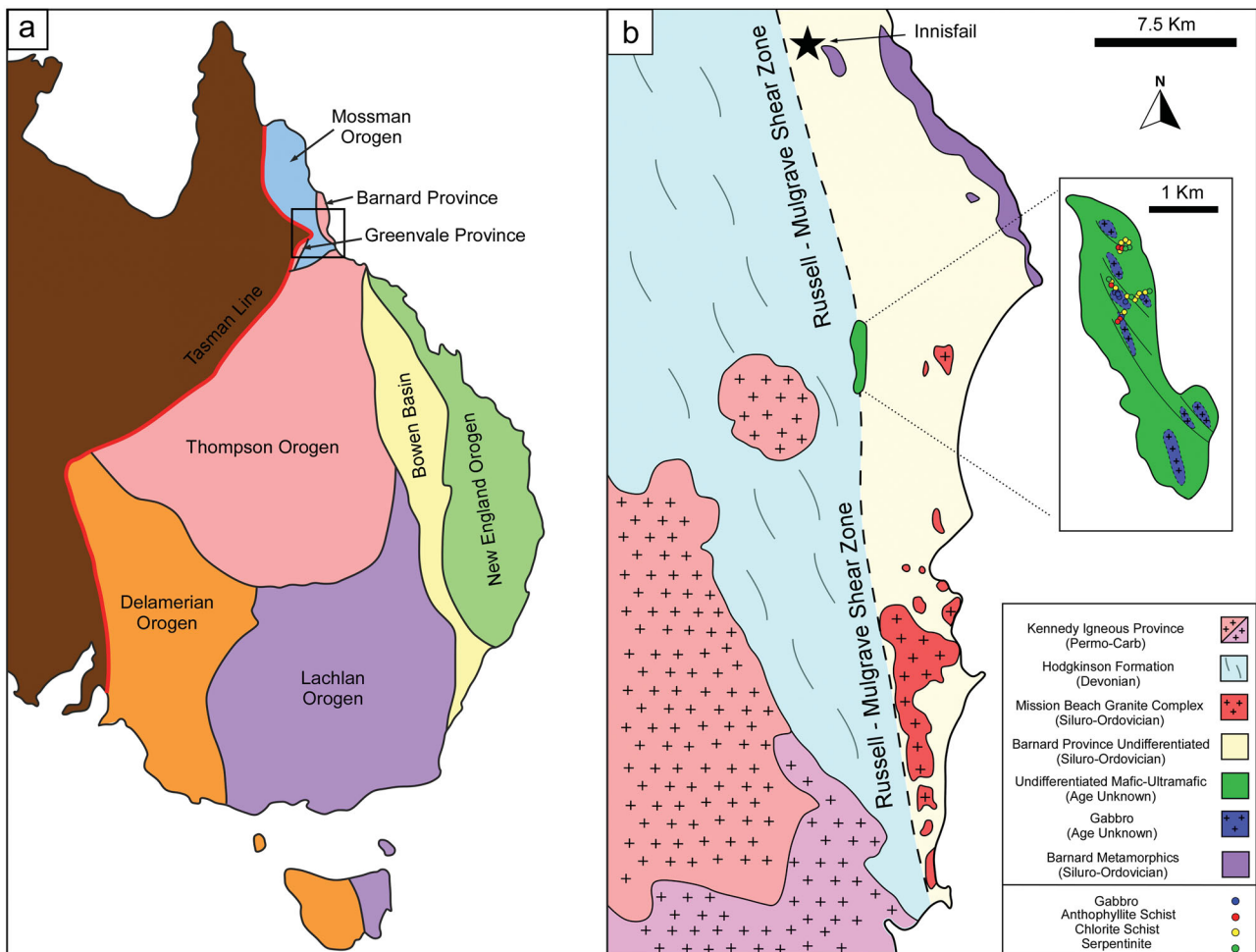


Figure 1. (a) Tectonic framework of the Tasmanides in eastern Australia after Glen (2013). The black box indicates the study area, which covers the Barnard Province and southeastern Mossman Orogen. (b) Local geology of the study area highlighted in (a) and the geology of the Cowley Ophiolite Complex (inset) with sample locations. Local geology after Langbein (2010).

extension of the Tasmanides. The Mossman Orogen is mainly composed of Ordovician–Devonian, marine, volcano-sedimentary turbidite sequences, which were deformed and metamorphosed up to greenschist facies during the late Devonian Tabberabberan Orogeny (*ca* 400–365 Ma; Henderson & Fergusson, 2019). Rocks of the Mossman Orogen lack the deformation fabrics of the older Benambran Orogeny (*ca* 450–400 Ma) that affected much of the Thomson Orogen. The Mossman Orogen has been subdivided into the southern Broken River Province and the northern Hodgkinson Province. The Broken River Province is characterised by variably deformed, Ordovician–Silurian volcano-sedimentary sequences (Vos *et al.*, 2005), with extensive turbidite successions and tectonic melange (Henderson & Fergusson, 2019). This sequence was interpreted by Henderson and Fergusson (2019) to have been deposited along an active subduction margin, in an evolving forearc basin, with deposition spanning 130 million years. Subsequent Devonian, compressional orogenesis resulted in deformation of the basin sequences.

The Silurian–Carboniferous Hodgkinson Province is the largest sub-unit in the Mossman Orogen. It extends north–

south for >500 km, and east–west from the coast to the Palmerville Fault (Withnall & Cranfield, 2013). The Hodgkinson Province consists mainly of marine siliciclastic sediments, with mafic volcanic units and fossiliferous limestone more common in the western successions (Bultitude *et al.*, 1990; Poblete *et al.*, 2021). Folding and thrusting events have disturbed much of the stratigraphy within the Hodgkinson Province. The major lithological units in the province are exposed along north–south-trending, thrust-bound belts, which comprise, from east to west, the Hodgkinson Formation, Chillagoe Formation, Mountain Creek Conglomerate, Mulgrave Formation and the Quadroy Conglomerate (Bultitude *et al.*, 1990). The tectonic setting of the Hodgkinson Province remains enigmatic. An investigation of basalt geochemistry by Vos *et al.* (2006) concluded that the Hodgkinson Province formed within an evolving backarc setting, with extension driven by the eastward retreat of an outboard subduction complex. Other authors have suggested formation within a forearc setting associated with oblique slip subduction (Henderson, 1980, 1987), or a continental margin rift setting (Garrad & Bultitude, 1999).

The Hodgkinson Formation is the most widespread unit in the Hodgkinson Province. It mostly consists of turbidite sequences and tectonic melange, with minor volcanic intercalations and pelagic sediments (Davis *et al.*, 2002). Zucchetto *et al.* (1999) described the Hodgkinson Formation as having undergone four deformational events (D1–D4). D1 involved the formation of melange through the inclusion of meta-arenite clasts in a meta-pelitic matrix. D2 is characterised by a steeply dipping pervasive cleavage, and tight, moderately to steeply plunging folds at decimetre to kilometre scales that resulted from east–west shortening. The effects of the D3 event are best visible in thin-section and are characterised by the development of S3. S3 is marked by cleavage intensification and phyllosilicate concentration, which developed at a low angle to S2, and its formation has been attributed to sub-horizontal shortening (D3). D4 events were associated with the formation of the dominant foliation, S4, which developed throughout the Hodgkinson Formation, and trends north-northwest/south-southeast. S4 is roughly coplanar to lithological layering, the melange foliation and the axial plane of mesoscopic folds, and has been attributed to the reactivation of S2 (Zucchetto *et al.*, 1999).

Along its southeastern margin, the Hodgkinson Formation is in faulted contact with the Siluro-Ordovician Barnard Metamorphics. De Keyser (1965) interpreted the Barnard Metamorphics as higher-grade, metamorphic equivalents of the Hodgkinson Formation, but Garrad and Bultitude (1999) suggested that the Barnard Metamorphics likely represent Paleozoic basement to the Hodgkinson Formation. More recent work by Betts *et al.* (2012) described the Barnard Metamorphics as a ribbon continent that formed following backarc basin rifting owing to the eastward migration of a westward-dipping Paleozoic subduction complex. The Russell-Mulgrave Fault separates the Hodgkinson Formation to the west from the Barnard Metamorphics to the east, and it extends from Tully to the north of Cairns. The COC is situated along the Russell-Mulgrave Fault, and it represents one of many occurrences of ultramafic rocks along this boundary.

Methods

Forty-five samples of mafic and ultramafic rocks were collected from the COC to conduct whole-rock, major- and trace-element geochemistry, prepare and describe petrographic thin-sections, and obtain high resolution mineral chemistry data. Major- and trace-element, whole-rock geochemistry was undertaken externally by Bureau Veritas, in Vancouver, Canada. Petrographic thin-sections were prepared at Ingham Petrographics and analysed at James Cook University. Ultramafic schist samples were categorised by dominant mineralogy and major-element chemistry. Fifty-one major-element analyses for chromite were collected on the JEOL JXA 8200 Electron Probe Micro Analyser (EPMA) at the Advanced Analytical Centre, James Cook University, using an acceleration voltage of 15 kV, 2 nA probe current and probe diameter of 5

microns. The oxides that were analysed included Al_2O_3 , Cr_2O_3 , FeO, MgO, ZnO, V_2O_5 , NiO and TiO_2 .

Rock types of the COC

The COC comprises a range of mafic–ultramafic lithologies including gabbro, serpentinite, chlorite schist and anthophyllite schist (Figure 2). Alteration was observed in all samples, and ranges from hydration of primary pyroxenes and amphiboles to form secondary amphiboles in gabbro, to the complete replacement of primary minerals such as in serpentinite, chlorite schist and anthophyllite schist (Figure 2c, j). The COC is crosscut by numerous moderately steeply eastward-dipping shear zones. The distribution of gabbro, ultramafic schist varieties and alteration assemblages is spatially related to these shear zones. However, the timing relationship between the intrusion of the gabbro and the shear zone development is unclear.

Gabbro is common throughout the COC. It is black, green and white in colour, displays a well preserved, equigranular, coarse-grained igneous texture and outcrops as blocky masses along the crest and eastern side of the complex. The gabbro is hornblende dominant, with minor clinopyroxene and variable amounts of plagioclase. Hornblende and clinopyroxene commonly display partial or complete replacement by anthophyllite and tremolite, and varying degrees of chlorite–vesuvianite–carbonate alteration and veining.

Serpentinite lenses occur throughout the COC and contain varying proportions of serpentine, talc, chlorite, and opaques (Figure 2e–g). They are typically dark green in colour, but may oxidise to a reddish-brown colour or display vibrant green colours where Ni-carbonates are present. Talc-rich varieties are black in colour and soapy to touch, but are less common. The serpentinite rocks are generally fine-grained, but some varieties contain coarse-grained, fibrous serpentine minerals. Opaques minerals, including magnetite, ilmenite, hematite, and chromite, are common in variable proportions and as veinlets. The serpentinisation of primary silicate minerals in these rocks has been complete. However, relict grain boundaries have been preserved to reflect the existence of earlier, coarse-grained peridotite textures in many samples.

Chlorite schist is the most abundant rock type observed within the COC. It contains >90% chlorite with accessory talc, serpentine, and opaques (Figure 2a–d). Chlorite schist is dark green to black in colour, fine- to medium-grained and commonly deeply weathered to a clay. Primary minerals were replaced by chlorite, but relict grain boundaries are preserved. The chlorite schist is spatially related to the numerous shear zones that crosscut the complex. Monomineralic chlorite schist in ultramafic complexes have been termed ‘blackwall’ metasomatic alteration fronts (Brown *et al.*, 2020; Spandler *et al.*, 2008).

Anthophyllite-bearing schist occurs as small lenses throughout the COC. Samples were taken from subcrops, and field relationships to the other lithologies are unclear.

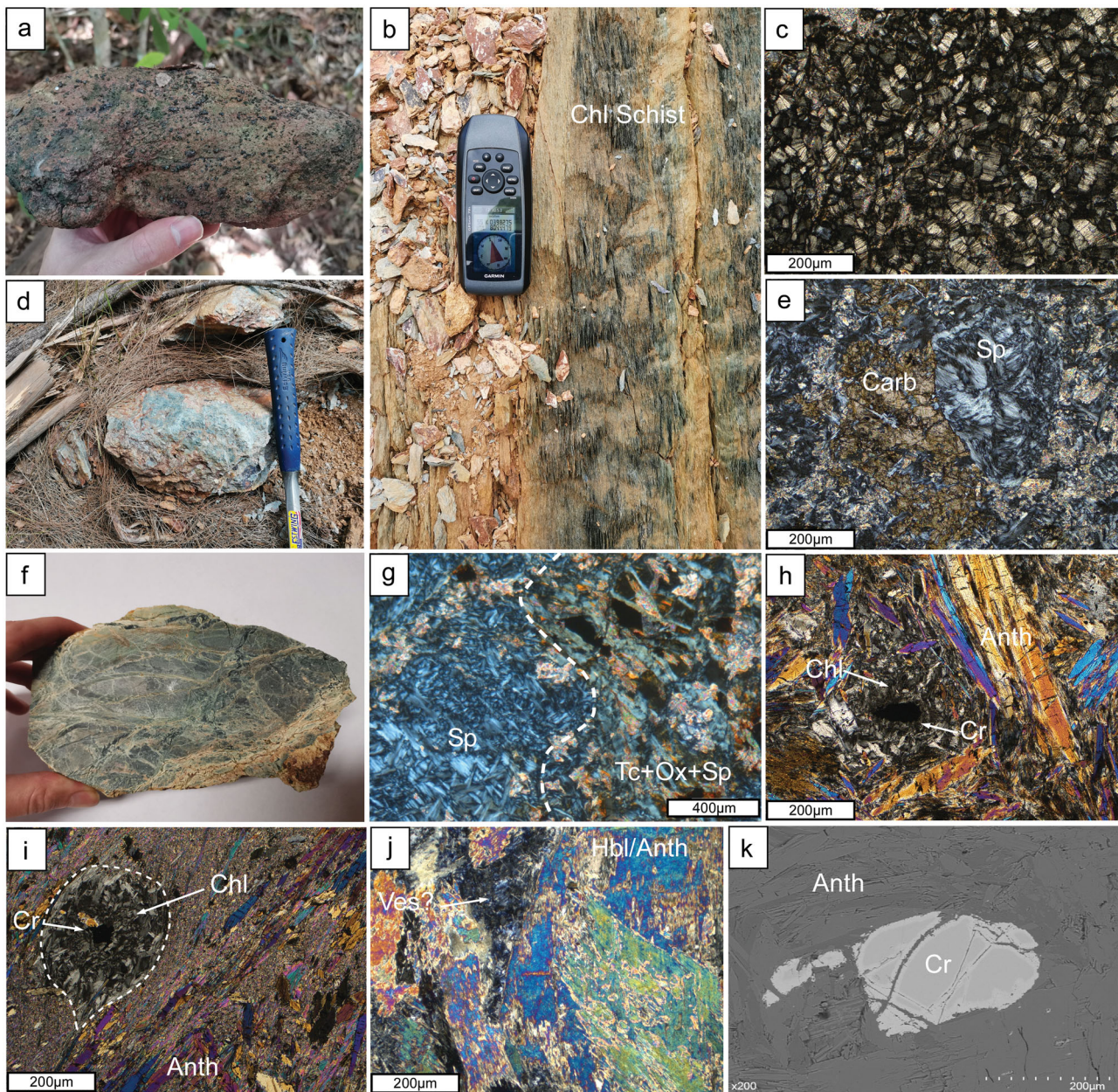


Figure 2. Compilation of field photographs and photomicrographs from the COC. (a) Chlorite schist with abundant, large secondary magnetite crystals. (b) Intense chlorite alteration ('blackwall' alteration) occurring along a steeply east-dipping thrust zone. (c) Photomicrograph showing complete chloritisation of protolith peridotite. Relict, equigranular grain textures have been retained. (d) Deeply weathered chlorite schist. (e) Photomicrograph of a Mg-rich serpentine (fibrous) carbonate–talc altered rock. Alteration was texturally destructive. (f) Serpentinised ultramafic rock from the COC. Multiple generations of crosscutting veins contain serpentine minerals. (g) Photomicrograph depicting multiple serpentine generations. An earlier assemblage of talc–oxide–serpentine (right side) is progressively overprinted by massive serpentine (left side). The dotted line tracks the alteration front of the later serpentinisation event. (h, i) Photomicrographs of anthophyllite schist characterised by elongate, prismatic anthophyllite grains that surround porphyroclasts, replaced by chlorite, with cores of chromite. (j) Coarse-grained hornblende gabbro. Hornblende is partly replaced by anthophyllite or tremolite. Interstitial berlin blue mineral may be vesuvianite. (k) Backscatter image of a zoned (altered) chromite grain surrounded by prismatic anthophyllite. Chromite alteration is late and fracture-controlled, and its formation does not reflect a primary magmatic process.

The anthophyllite schist is light green in colour and comprises anthophyllite and chromite, with crosscutting carbonate veinlets (Figure 2h, i). Some varieties are intensely sheared, and contain pseudo-morphed porphyroclasts of chlorite, that surround chromite (Figure 2i). The anthophyllite grains are typically euhedral, coarse-grained and fibrous-prismatic. The anthophyllite replaced the primary minerals and is texturally destructive.

Whole-rock geochemistry

The SiO_2 and Al_2O_3 content in gabbro ranges from 42–52 wt% and 14–19.5 wt%, respectively, with SiO_2 decreasing with increasing MgO (Figure 3). The total FeO ranges from 4.3–7.7 wt% and correlates positively with increasing MgO (9.3–13.5 wt%), whereas Na_2O (0.3–3 wt%) shows a strong negative correlation with increasing MgO.

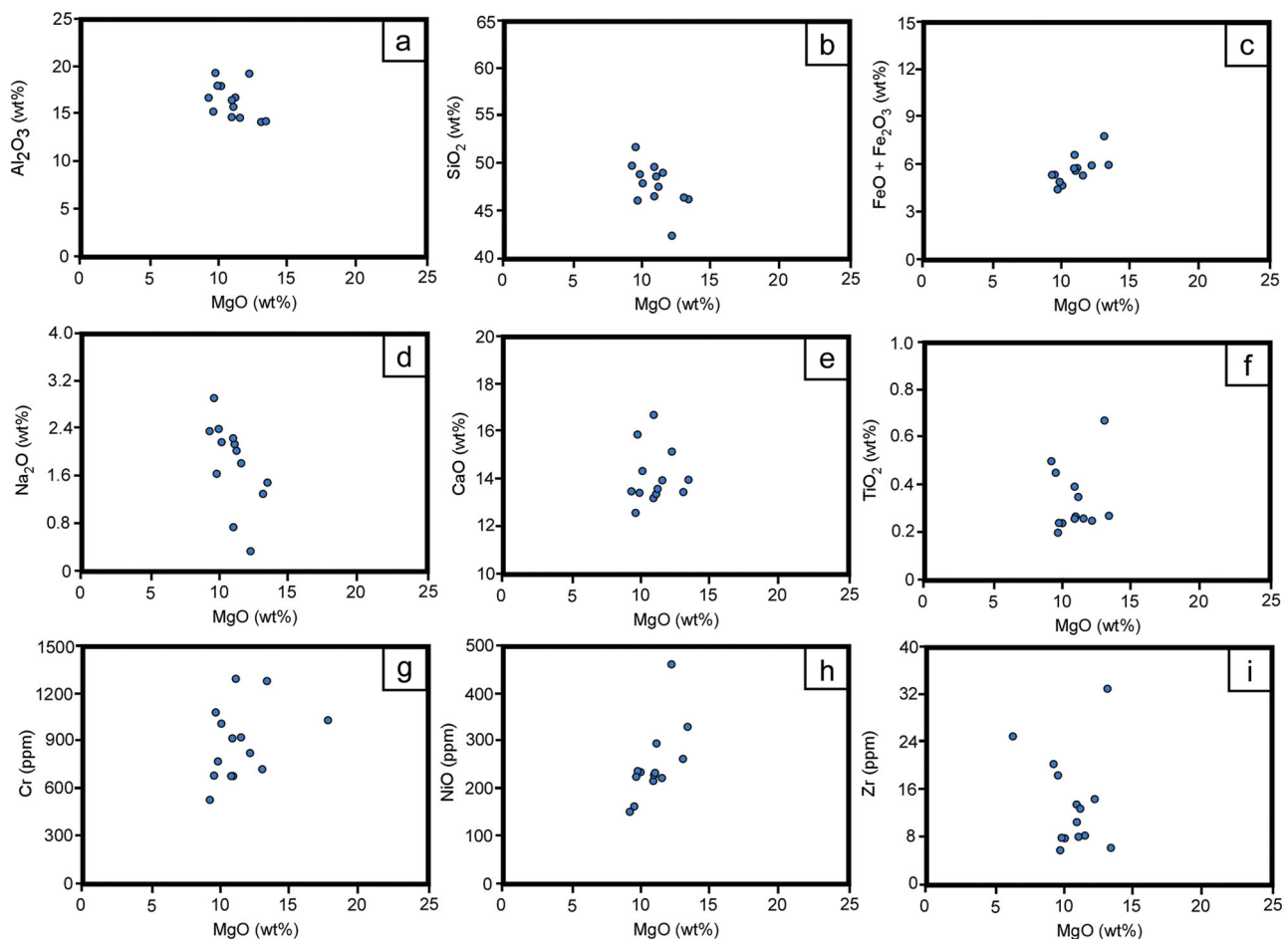


Figure 3. Major and trace elements vs MgO (wt%) for the gabbro samples collected from the Cowley Ophiolite Complex.

CaO (12.5–16.7 wt%) and TiO_2 (0.2–0.7 wt%) do not show obvious trends as a function of MgO content, whereas Cr (533–1286 ppm) and Ni (150–462 ppm) display strong positive correlations with MgO content. Major- and trace-element discrimination plots (Figure 4) can be used to classify the gabbro as sub-alkaline to calc-alkaline, and island-arc tholeiite. Primitive mantle normalised rare earth elements (REE) patterns (Figure 5) of the gabbro display flat light REE (LREE) and heavy REE (HREE) compositions, with weak Eu anomalies. Two samples contain higher total REE (TREE) concentrations, but with similar flat distribution patterns.

Two populations of chlorite schist can be defined based on major-element chemistry (Figure 6). A first population contains low SiO_2 (28–33 wt%), TiO_2 (0–1 wt%), Na_2O , K_2O and CaO (<0.1 wt%), high MgO (26–29 wt%), Al_2O_3 (17–22 wt%) and FeO (7–12 wt%). A second population contains lower SiO_2 (24–32 wt%) and MgO (20–26 wt%), low CaO (0–0.13 wt%), Na_2O and K_2O (<0.1 wt%), with high Al_2O_3 (14–21 wt%), higher FeO (9–25 wt%) and TiO_2 (0.5–2.5 wt%). The Ni and Cr content are variable with 265–2032 ppm Ni and 260–2970 ppm Cr. The chlorite schist samples display flat REE patterns, normalised to primitive mantle, with distinct Ce and Eu depletion (Figure 5) and

generally contain greater TREE concentrations than the anthophyllite schist and serpentinite samples.

Compared with the other ultramafic schist varieties, the anthophyllite schist contains high SiO_2 (39–55 wt%) and CaO (3–11 wt%), moderate Al_2O_3 (2–11 wt%) and MgO (21–26 wt%), and low TiO_2 (0–0.3 wt%), FeO (5–10 wt%), Na_2O (0–0.05 wt%) and K_2O (<0.01 wt%) (Figure 6). The anthophyllite schist samples are relatively Ni-rich (965–2097 ppm) and have a variable Cr content (342–3161 ppm). In primitive mantle normalised REE plots, anthophyllite schist displays mixed patterns with variable positive and negative Ce and Eu anomalies, but with overall flat LREE/HREE ratios (Figure 5) and similar TREE concentrations as the serpentinite samples.

Two populations of serpentinite can be defined based on their MgO content (Figure 6). Population 1, which consists of four samples, contains high SiO_2 (47–58 wt%), moderate MgO (26–27 wt%), and low Al_2O_3 (2 samples at 0.5–2 wt%, and two samples at 8–9 wt%), FeO (7–9 wt%), TiO_2 (0–0.16 wt%), CaO (0–0.3 wt%), Na_2O and K_2O (<0.01 wt%). Population 1 contains high Ni (1375–2353 ppm) and moderate Cr (1500–2573 ppm) when compared with the chlorite schist and anthophyllite schist samples. Population 2, which consists of two samples, contains a similar major-element

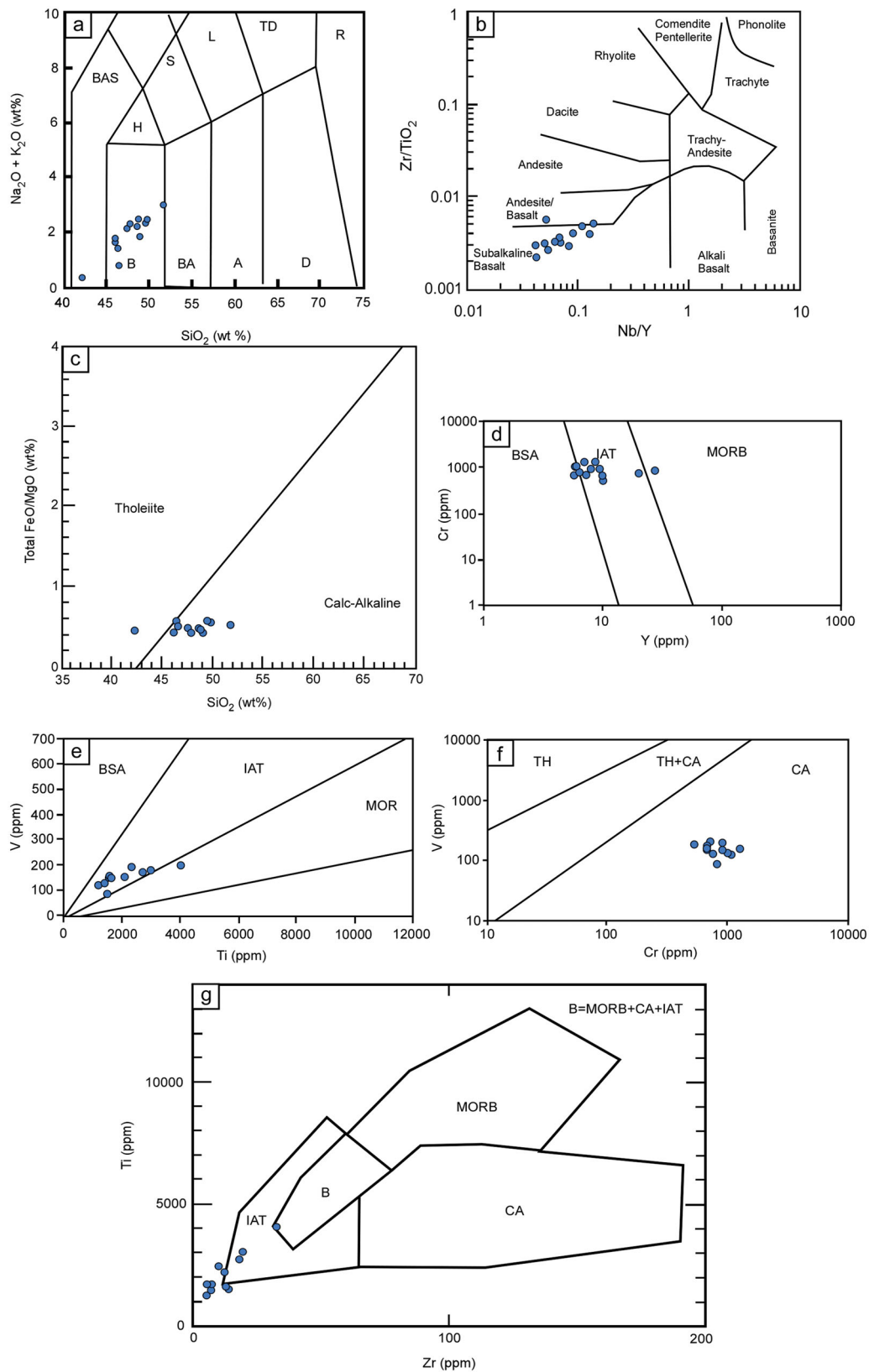


Figure 4. Geochemical, tectonic discrimination plots for the gabbro collected from the Cowley Ophiolite Complex. The gabbro is basaltic in composition and typically plots within island arc tholeiite (IAT) and calc-alkaline (CA) compositional fields. (a) Total alkali silica (TAS) plot after Middlemost (1994). (b) Zr/TiO_2 vs Nb/Y fields after Winchester and Floyd (1977). (c) FeO/MgO vs SiO_2 fields after Miyashiro (1974). (d) Cr vs Y fields after Yellappa *et al.* (2010) modified after Pearce *et al.* (1981). (e) V vs Ti fields after Shervais (1982). (f) V vs Cr fields after Miyashiro and Shido (1975). (g) Zr vs Ti fields after Pearce and Cann (1973).

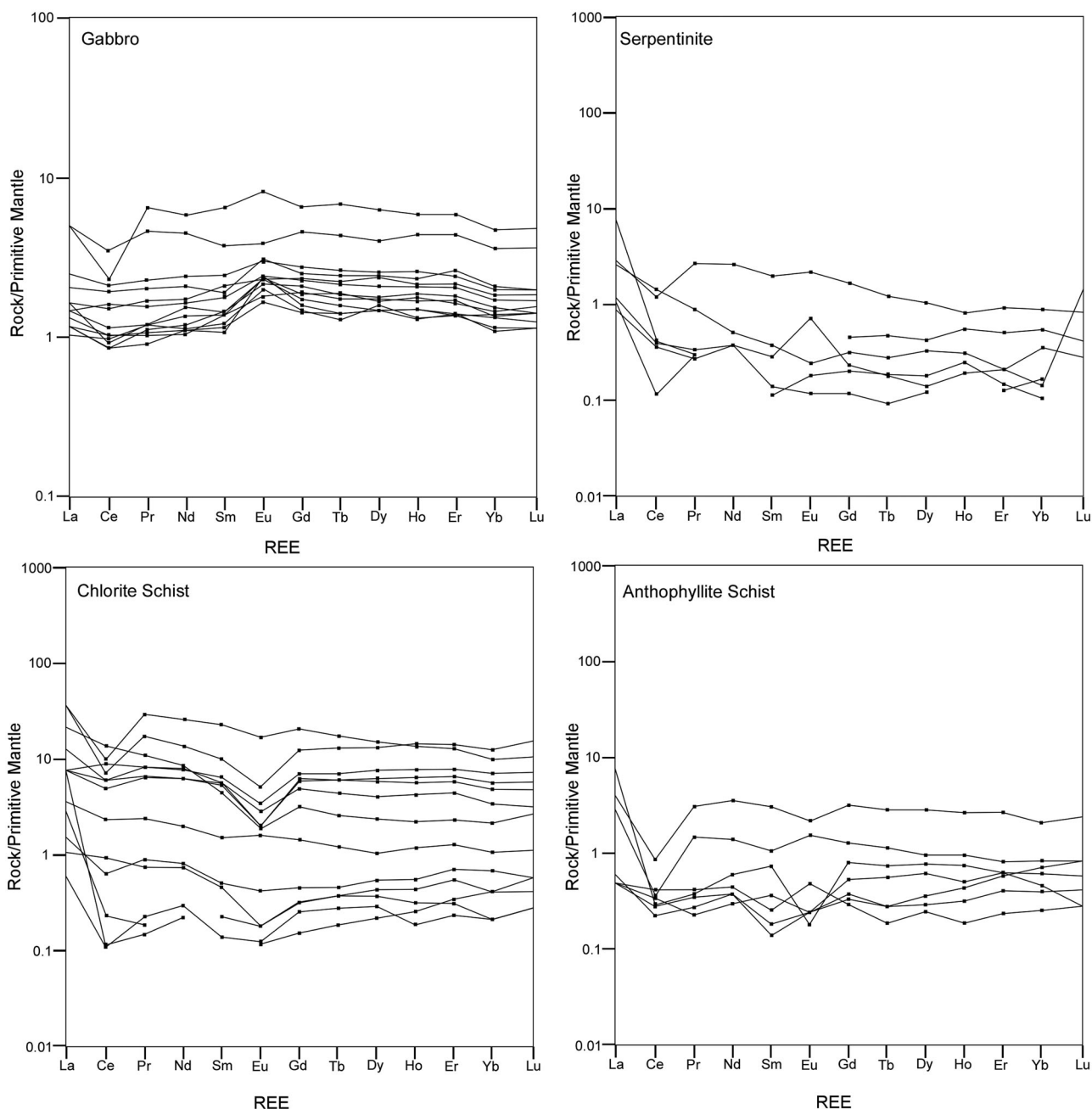


Figure 5. Primitive mantle normalised REE patterns for the gabbro, serpentinite, chlorite schist and anthophyllite schist. Normalising values are from O'Neill and Palme (2014).

chemistry to population 1 except for higher MgO (35–36 wt%), Ni (2163–2273 ppm) and Cr (2299–3578 ppm) content, and lower SiO₂ (40–43 wt%). The serpentinites display flat primitive mantle normalised, REE patterns, with a variable Ce anomaly and no Eu anomaly. The TREE concentration is similar to that in the anthophyllite schist samples.

Chromite chemistry

Chromite grains from chromite-bearing anthophyllite schist samples were analysed to fingerprint the tectonic setting

and petrogenetic history of the COC. Fifty-one analyses of chromite were taken from two anthophyllite schist samples. Individual chromite grains preserve distinct core and rim compositions. Chromite cores contain 35–45 wt% Cr₂O₃, 13–20 wt% Al₂O₃, 27–40 wt% FeO, 0.8–4 wt% MgO (outlier at 8.2 wt%), 0.7–4.7 wt% ZnO, 0–4 wt% TiO₂, Cr# 57–67 and Mg# 5–20 (an outlier at Mg# 47) with trace NiO (0–0.15 wt%) and V₂O₃ (0–0.6 wt%). The chromite rims contain 33–46 wt% Cr₂O₃, 1–9 wt% Al₂O₃, 29–55 wt% total FeO, 0.3–0.8 wt% MgO (outlier at 2.12 wt%), 0.4–3.5 wt% ZnO, 0.3–4.04 wt% TiO₂, 0.28–0.56 wt% V₂O₃ and 0.03–0.14 wt% NiO. Chromite rims have a Cr# of 78–94, and a Mg# of 1–13.

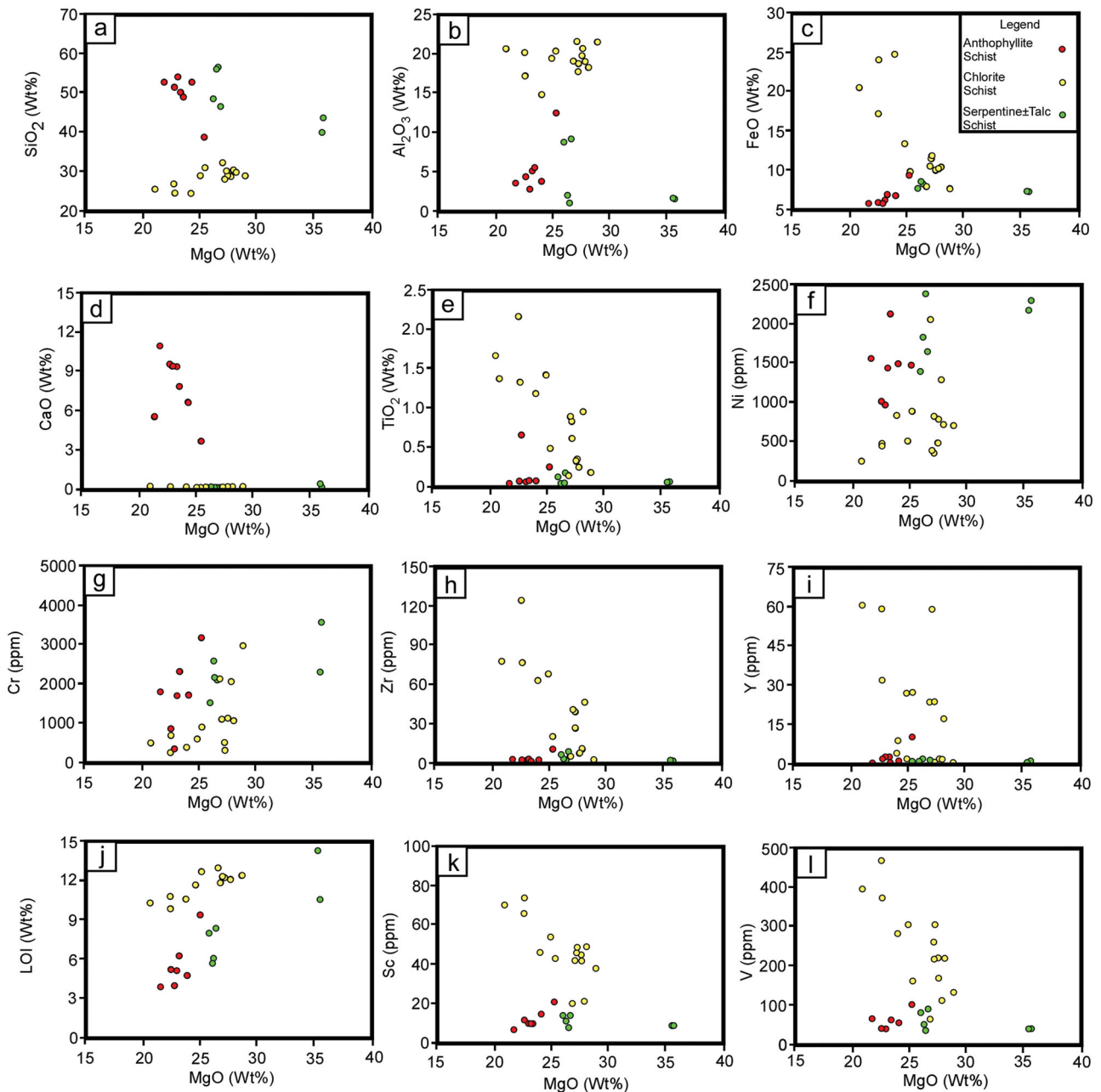


Figure 6. Plots of major and trace elements vs MgO (wt%) for the serpentinite (green symbols), chlorite schist (yellow symbols) and anthophyllite schist (red symbols) samples collected from the Cowley Ophiolite Complex.

The Cr# vs Mg# petrogenetic discrimination plot (Figure 7a), first presented by Dick and Bullen (1984), is a commonly used geochemical tool to differentiate chromite formed within stratiform complexes, Alaskan-style intrusive complexes, alpine peridotite and abyssal peridotite. Chromite cores and rims from the COC mostly plot outside the known compositional fields (Figure 7a), but display a strong, linear, positive correlation between increasing Cr# and decreasing Mg# across both the core and the rim compositions.

The TiO₂ vs Al₂O₃ geochemical, discrimination plot (Figure 7b) after Kamenetsky *et al.* (2001) can be used to characterise spinels that formed within various tectonic settings including arcs, large igneous provinces and subduction

complexes. The analyses of chromite cores from the COC plot as two populations that belong to individual samples. Chromite cores from sample C18 plot mostly within the supra-subduction zone field, whereas chromite cores from sample C26 plot within the supra-subduction zone and ocean island basalt (OIB) fields. The chromite rims also plot as two distinct populations. The chromite rims from sample C18 plot within the 'high Ti arc' field, whereas the chromite rims from sample C26 plot outside the discriminatory fields. The chromite rims from both samples show reduced Al concentrations relative to the chromite cores.

The ratios of 3⁺ cations (Al, Cr and Fe³⁺) are used to classify spinel minerals, and to discriminate their petrogenetic

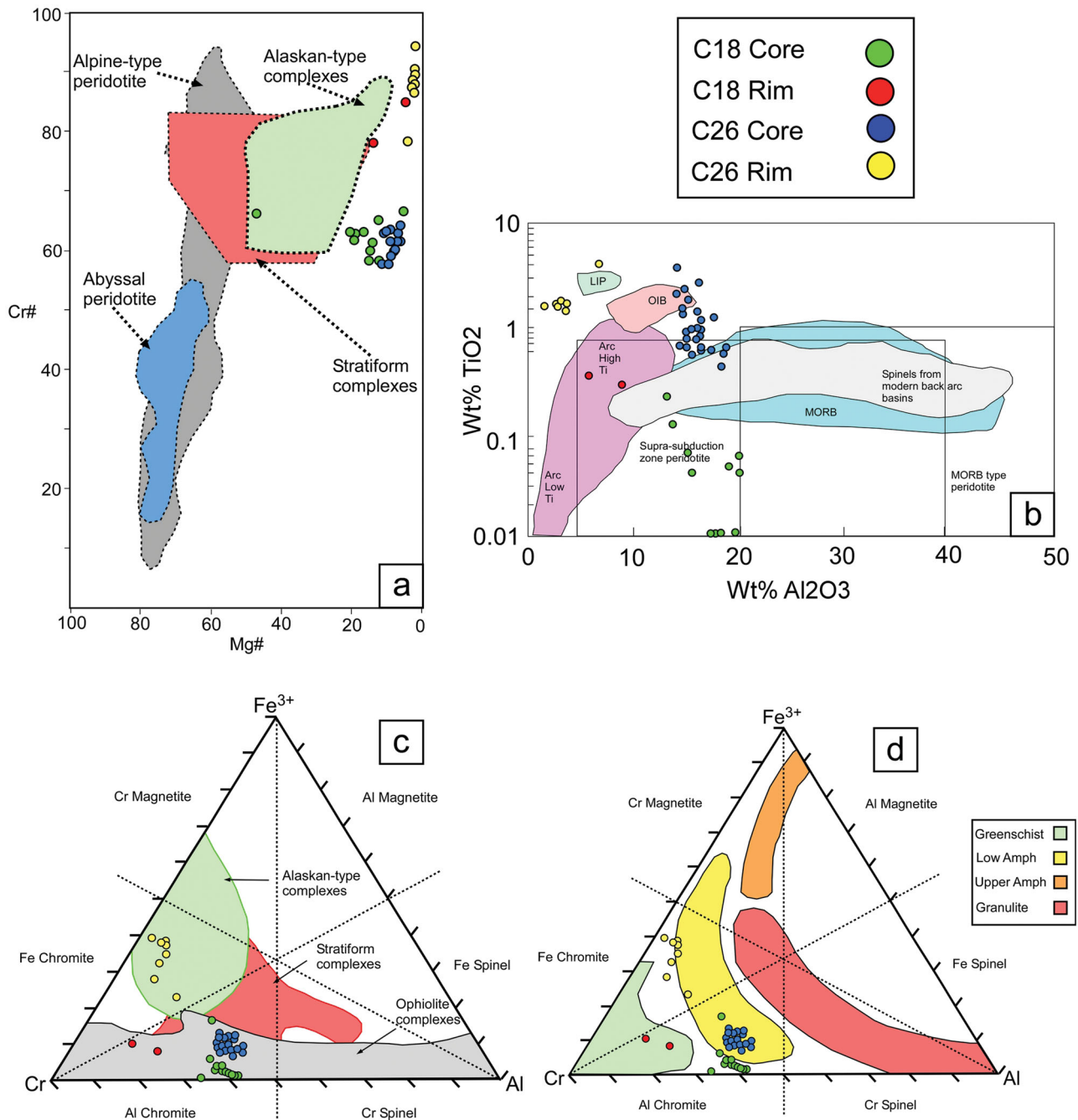


Figure 7. Geochemical, tectonic discrimination plots of chromite hosted within the COC anthophyllite schist. (a) Cr# vs Mg# fields after Dick and Bullen (1984). (b) TiO₂ vs Al₂O₃ fields after Kamenetsky *et al.* (2001) and Ishwar-Kumar *et al.* (2018). (c) 3⁺ cation ternary diagram tectonic discrimination fields after Barnes and Roeder (2001) and Yu *et al.* (2019). (d) 3⁺ cation ternary diagram metamorphic facies discrimination after Proenza *et al.* (2008).

setting (Barnes & Roeder, 2001; Proenza *et al.*, 2008). The chromite cores of both samples from the COC plot within the Al-chromite field, whereas the chromite rims plot within both the Al-chromite (sample C18) and Fe-chromite (sample C26) fields. The chromite cores from both samples plot within the ophiolite complex field (Figure 7c). The chromite rims from sample C18 plot within the ophiolite complex field, whereas the chromite rims from sample C26 plot mostly within the stratiform complex field. The chromite cores from both samples plot either within, or just outside, the lower amphibolite facies metamorphism field (Figure

7d). The chromite rims from sample C18 plot within the greenschist facies metamorphism field, whereas the chromite rims from sample C26 plot either within, or just outside, the lower amphibolite facies metamorphism field.

Discussion

Alteration and the tectonic setting of the COC

The ultramafic rocks observed within the COC record three distinct styles of alteration: chlorite 'blackwall' alteration,

anthophyllite alteration and serpentinitisation. Carbonate veining and carbonate alteration accompany the anthophyllite alteration and serpentinitisation. From the alteration assemblage, and the chemistry of the gabbro, we can infer the tectonic setting during alteration, the metamorphic conditions during alteration, the ultramafic protolith lithologies and the chemistry of the fluid responsible for the alteration. Monomineralic chlorite schist, which is commonly referred to as blackwall alteration, is an alteration style that has been attributed to subduction zones, and oceanic core complex settings (Boschi *et al.*, 2006; King *et al.*, 2003; Spandler *et al.*, 2008). Blackwall alteration has been interpreted to form by fluid–rock interaction between an ultramafic protolith, and a pervasive, metasomatic or hydrothermal fluid, derived, in part, from seawater. Blackwall alteration is commonly observed proximal to shear zones (Spandler *et al.*, 2008). The blackwall alteration, observed throughout the COC, is indicative of the circulation of hydrous fluids. These fluids were potentially sourced from either the infiltration of seawater into upper mantle peridotite within an oceanic extensional setting (Boschi *et al.*, 2006; Schroeder & John, 2004), or from connate fluids and structural hydroxyl that was liberated during dehydration reactions associated with slab subduction and prograde metamorphism (Zheng *et al.*, 2016). The infiltration of subduction-related hydrous fluids, derived from seawater, is consistent with the weakly negative Ce anomalies of the COC gabbro samples (Figure 5), which in island-arc mafic rocks have been attributed to the subduction of pelagic sediment, and fluid mobilisation (Hole *et al.*, 1984). Furthermore, the lack of negative Eu anomalies from the COC gabbro samples may suggest the suppression of plagioclase fractionation owing to the influx of strongly hydrous fluids (Müntener *et al.*, 2001). The buoyancy-driven ascent of these subduction derived fluids resulted in metasomatic alteration of the overriding mantle wedge within a forearc/supra-subduction zone setting (Abuamarah *et al.*, 2020; Berly *et al.*, 2006). The gabbro from the COC has a calc-alkaline, island-arc tholeiitic, geochemical affinity (Figure 4), which has been attributed to rocks formed within a supra-subduction zone during the transition from tholeiitic to calc-alkaline compositions (Belyaev *et al.*, 2021). Similarly, island-arc tholeiitic gabbro from ophiolite belts has been commonly interpreted to have formed by intra-oceanic subduction and island-arc formation (Buckman *et al.*, 2018; Manton *et al.*, 2017; Yellappa *et al.*, 2010). The gabbro recorded the alteration of pyroxene to secondary magnesio-hornblende and anthophyllite/tremolite, which may suggest that the intrusion of the gabbro pre-dated the alteration of the complex. Therefore, owing to the widespread blackwall alteration of the ultramafic rocks, and the geochemistry of the gabbro, we prefer an interpretation in which the COC was generated within a forearc/supra-subduction zone setting.

The COC records a higher grade of metamorphism than the surrounding Hodgkinson Formation, which has been

interpreted to have experienced greenschist facies metamorphism (Henderson *et al.*, 2013). Abdel-Karim *et al.* (2016) described anthophyllite schist as the alteration product of a pyroxenitic protolith. Anthophyllite is generally considered to form at temperatures above 600 °C, and it has been interpreted as a retrograde alteration product in ultramafic rocks that record amphibolite facies metamorphism (Yu *et al.*, 2019). The anthophyllite alteration of ultramafic rocks observed within the COC constrains minimum temperature conditions to >600 °C, and the presence of anthophyllite–talc has been interpreted to constrain temperature conditions to 400–700 °C (Yu *et al.*, 2019), typical for amphibolite facies metamorphism.

The variety of alteration assemblages observed within the COC probably reflects mineralogical variation within the ultramafic protoliths. Blackwall alteration and anthophyllite alteration commonly occur within a pyroxenite protolith (Abdel-Karim *et al.*, 2016; Rinne & Hollings, 2013; Takla *et al.*, 2004). Serpentinitisation may affect a range of ultramafic protoliths from pyroxenite to dunite, and these can be distinguished geochemically (Deschamps *et al.*, 2013). The blackwall-style alteration, and elevated Sc content (Figure 6k), of the chlorite schist from the COC, most likely indicates a pyroxenite protolith (Wang *et al.*, 2021). Compared with the chlorite schist, the anthophyllite schist contains more Ni, less Sc (Figure 6) and approximately the same amount of MgO and may reflect a more olivine-rich protolith to the anthophyllite schist, such as harzburgite. Samples of serpentinite from the COC display significant variability in their major- and trace-element composition. On average, the samples containing lower MgO also contain less Ni. This may indicate the presence of two protoliths to the serpentinite; a more olivine-rich variety, possibly a dunite, containing higher MgO and Ni, and a less olivine-rich variety, possibly a harzburgite, containing less MgO and Ni. The variation in alteration, which we infer to reflect mineralogical variation within the ultramafic protolith, indicates that the COC was a differentiated mafic–ultramafic complex.

Chromite chemistry

The major- and trace-element chemistry of chromite can be used to constrain the tectonic setting, petrogenesis and alteration history of ultramafic complexes (Arif & Jan, 2006; Barnes, 2000; Dick & Bullen, 1984; Gamal El Dien *et al.*, 2019; Irvine, 1965; 1967; Wang *et al.*, 2005). Chromite is typically more resistant to alteration than primary silicates, and is commonly the only relict primary phase within intensely altered mafic–ultramafic rocks (Zaccarini *et al.*, 2011).

The geochemical discrimination of the chromite from the COC (Figure 7) complements the findings and inferences made about the tectonic setting and petrogenesis of the COC, determined in the alteration study. However, the chromite grains, hosted within the anthophyllite schist from the COC, display evidence of metasomatic

modification. Chemical zonation associated with fractured chromite grains (Figure 2k) is consistent with the core–rim zonation observed in undeformed grains. Therefore, we interpret that the chemical zonation reflects the effects of metamorphism or metasomatic alteration, and not a primary magmatic process (Colás *et al.*, 2014; Jiménez *et al.*, 2009). The chemistry of chromite cores, which commonly record less metasomatic modification, display compositions consistent with a supra-subduction zone and an OIB signature (Figure 7b; Kamenetsky *et al.*, 2001). We interpret this signature to reflect the tectonic processes that occur along an active subduction margin. The subduction of oceanic lithosphere, potentially OIBs, beneath an overriding mantle wedge resulted in prograde dehydration reactions, which generated metasomatic fluids. These fluids most likely migrated through the overriding mantle wedge, where they metasomatised the peridotite within a supra-subduction zone setting. The ternary plots, which depict the ratio of 3^+ cations in chromite, suggest that the chromite records amphibolite facies metamorphism, and that they have an ophiolite origin (Figure 7c, d). The amphibolite facies metamorphic signature of the chromite cores complements the anthophyllite alteration, which is also consistent with amphibolite facies conditions. The ophiolite signature is consistent with our interpretation of a supra-subduction zone environment. Supra-subduction zones are the most common tectonic setting in which ophiolites have been described (Shervais, 2001).

Tectonic implications

We interpret the COC as a differentiated mafic–ultramafic complex that was metasomatised under at least amphibolite facies metamorphic conditions, within a supra-subduction zone setting. The COC is positioned along the Russell-Mulgrave Fault, and records higher-grade metamorphism than the surrounding Hodgkinson Formation (Henderson *et al.*, 2013). The Russell-Mulgrave Fault is a regional structure that marks the boundary between the Hodgkinson Province to the west, and the Barnard Province to the east (Figure 1b). Our interpretation of the alteration assemblages, and geochemistry, of the COC, suggests that the COC is most likely an ophiolite complex that was emplaced along an active subduction margin. We propose that this ancient subduction margin is now represented by the Russell-Mulgrave Fault.

We interpret that metamorphism and emplacement of the COC pre-dated the deposition of the Hodgkinson Formation, which is thought to have occurred within either a backarc (Garrad & Bultitude, 1999) or forearc environment (Henderson, 1980). The Barnard Metamorphics, situated to the east, have been interpreted as either a sequence of uplifted basement rocks (Bultitude *et al.*, 1997) or a continental ribbon that was rifted from the Australian continent during backarc extension, and later re-accreted during backarc closure along the Russell-Mulgrave Fault (Betts

et al., 2012). Rifting within a backarc setting, followed by subduction and backarc closure, along the Russell-Mulgrave Fault, would imply that the COC is younger than the Hodgkinson Formation. The Hodgkinson Formation shows no evidence of an amphibolite facies metamorphic overprint, and the COC shows no geochemical evidence of a backarc affinity. We propose that the COC is older than the Hodgkinson Formation, and we prefer the interpretation that the Hodgkinson Formation, and much of the greater Mossman Orogen, represents an evolving active margin succession (Henderson *et al.*, 2011).

The strong island-arc tholeiitic signature of the COC gabbro may indicate the presence of an outboard intra-oceanic island-arc related to the formation of the COC (Figure 8). Our interpretation of an active subduction complex, and a potential outboard intra-oceanic arc, which pre-dated the formation of the Mossman Orogen, suggests that the Russell-Mulgrave Fault is a Paleozoic, continental suture zone. The continental suturing event, which pre-dated the formation of the Mossman Orogen, involved the Barnard Metamorphics to the east, and the North Australian Craton to the west. This event followed a period of ocean closure, and potentially, intra-oceanic arc obduction (Figure 8). The post-collisional history of the region involved extension, possibly related to post-collisional orogenic collapse, and the deposition of the Hodgkinson Province sequences, which now conceal much of the Russell-Mulgrave Suture Zone. The Russell-Mulgrave Fault is the second structure in northeastern Queensland, next to the Clarke River Fault (Dirks *et al.*, 2021), where evidence of collisional tectonics has been observed (Edgar *et al.*, 2022). Both structures represent faulted contacts between rocks of the Mossman Orogen and the supposed Thompson Orogen.

Potential for mineralisation

Ophiolite complexes have the potential to host resources of critical metals, typically formed by magmatic (Shi *et al.*, 2012) or lateritic processes (Elias, 2002). The magmatic processes governing the formation of podiform chromite deposits have been widely debated (Lago *et al.*, 1982; Rollinson, 2005; Xiong *et al.*, 2015). Most models for podiform chromite deposits within supra-subduction zone, ophiolite complexes describe slab-derived, magmatic fluids interacting with the overriding mantle wedge. This process involved the melting of chrome-rich clinopyroxene and orthopyroxene, thus enriching the slab-derived melt in chromium, and results in the subsequent precipitation of chromitite during dunite crystallisation (Rollinson & Adetunji, 2013; Zhou & Robinson, 1997). However, these models cannot account for podiform chromite deposits with UHP mineral inclusions and exsolution (Xiong *et al.*, 2015), so additional processes are at play in some cases. We interpret that the COC developed within a supra-subduction zone environment, which is favourable for the formation of ophiolite-hosted, podiform chromite deposits. However, no podiform chromite or chromitite lenses

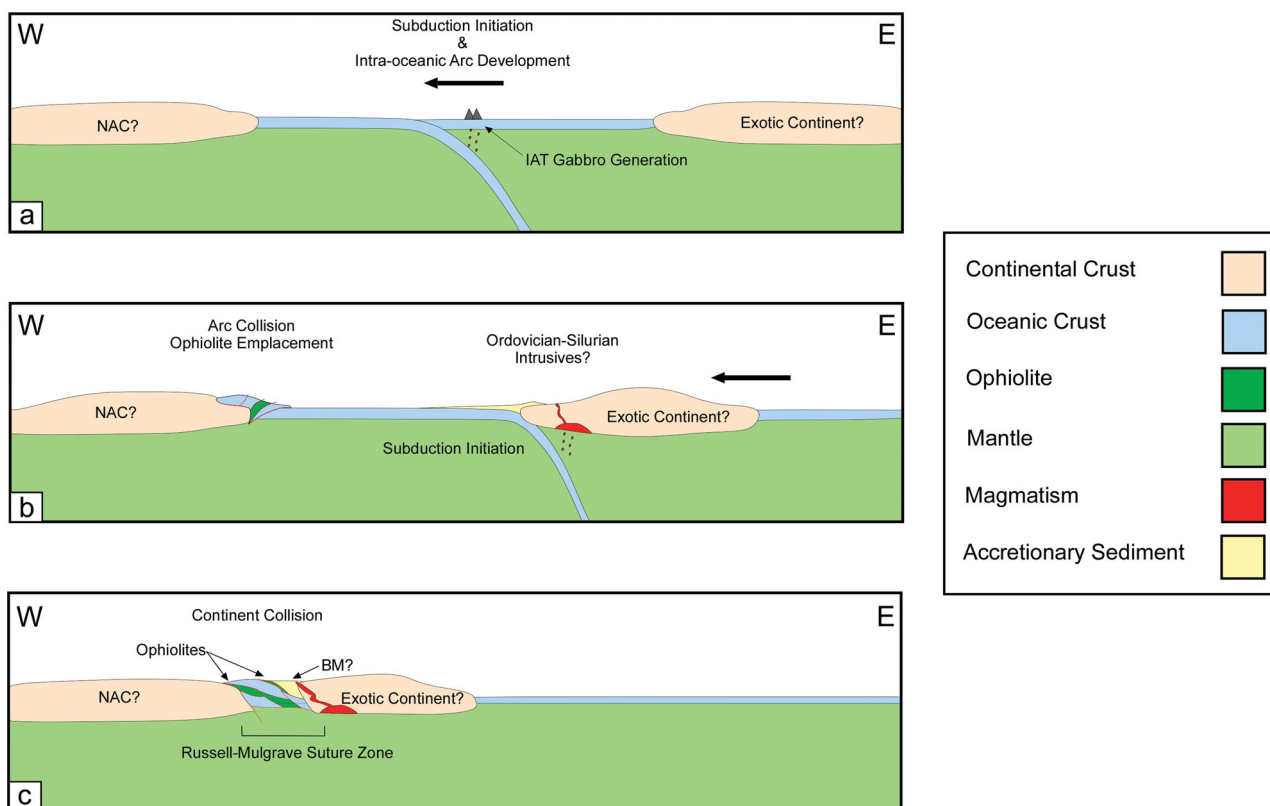


Figure 8. Tectonic model for depicting the formation and emplacement of the Cowley Ophiolite Complex. (a) An outboard, eastward-dipping subduction complex is responsible for the formation of an intra-oceanic, island-arc complex and the formation of island-arc tholeiitic (IAT) gabbro. (b) Slab rollback and westward migration of the intra-oceanic island-arc complex eventually results in arc accretion. Continuous convergence following subduction extinction along the North Australian Craton (NAC) results in eastward-dipping subduction initiation beneath an exotic continent or micro-continent. (c) Continuous westward retreat of the exotic continent results in collision, intense deformation of accreted sediments, possibly representing the Barnard Metamorphics (BM), and tectonic juxtaposition of ophiolite and sediment, marking the Russell-Mulgrave Suture Zone.

have been observed within the COC. The Cr grades in the whole-rock geochemistry of the ultramafic rocks that we have described do not exceed 3600 ppm and are sub-economic.

The ultramafic rocks observed within the COC are comparable with the bedrock lithologies that have been described from the Greenvale Ni–Co–Sc–Cr laterite deposits (Zeissink, 1969). Sc in ultramafic rocks is primarily hosted within clinopyroxene (Williams-Jones & Vasyukova, 2018). Consequently, pyroxenite has been recognised as a favourable host rock to primary, magmatic Sc mineralisation and secondary, laterite-hosted Sc mineralisation (Wang *et al.*, 2021). Ni laterite deposits are developed best on top of harzburgite and dunite. Ni preferentially partitions into olivine during the fractionation of ferro-magnesian magmas (Herzberg *et al.*, 2016); thus, olivine-rich peridotite generally contains greater concentrations of Ni. We have interpreted that, prior to alteration, the COC comprised differentiated peridotite, including pyroxenite and dunite. The COC contained bedrock lithologies that were favourable to the formation of lateritic Ni–Co–Sc–Cr deposits; however, we have not observed evidence for the development of a thick laterite profile in which leached metals could be concentrated into economically viable lodes.

Conclusions

The COC is a differentiated mafic–ultramafic ophiolite complex comprising gabbro, serpentinite, chlorite schist and anthophyllite schist. The alteration assemblage is indicative of subduction-related, hydrous, metasomatic fluids. Geochemical discrimination of the gabbro suggests a dominantly island-arc tholeiitic to calc-alkaline composition, which, in association with the subduction-related alteration, suggests a supra-subduction zone setting of formation. Geochemical discrimination of chromite suggests amphibolite facies metamorphic conditions, which is consistent with the formation of anthophyllite schist. We interpret that the COC was emplaced prior to the formation of the Mossman Orogen, and that the Russell-Mulgrave Fault represents an ancient subduction margin and continental suture zone. The COC contains favourable lithologies for the formation of lateritic deposits; however, evidence for such formations has not been observed.

Acknowledgements

The authors would like to thank Kevin Blake from the Advanced Analytical Centre at James Cook University (JCU) for his technical support during EPMA data collection and processing and Laurie Hutton

and Solomon Buckman for their reviews and constructive criticism of the original manuscript. Author contributions: AE and IS are responsible for conceptualisation, methodology, investigation, visualisation, supervision; AE wrote the original draft, and the writing, review and editing was carried out by all authors.

Disclosure statement

The authors declare that they have no known competing financial interests or personal relationships that could have appeared to influence the work reported in this paper.

Funding

The authors would like to thank the Geological Survey of Queensland for their funding of the project. The first author would like to acknowledge and thank JCU for the Australian Government Research Training Program (RTP) Domestic Stipend Scholarship, and the Economic Geology Research Centre (EGRU) at JCU for housing this research.

ORCID

A. Edgar  <http://orcid.org/0000-0002-8090-9788>
I. V. Sanislav  <http://orcid.org/0000-0002-3680-3740>
P. H. G. M. Dirks  <http://orcid.org/0000-0002-1582-1405>

Data availability statement

The authors confirm that the data supporting the findings of this study are available within the article or its [supplementary materials](#).

References

- Abdel-Karim, A-A M., Ali, S., Helmy, H. M., & El-Shafei, S. A. (2016). A fore-arc setting of the Gerf ophiolite, Eastern Desert, Egypt: Evidence from mineral chemistry and geochemistry of ultramafites. *Lithos*, 263, 52–65. <https://doi.org/10.1016/j.lithos.2016.05.023>
- Abuamarah, B. A., Asimow, P. D., Azer, M. K., & Ghrefat, H. (2020). Suprasubduction-zone origin of the podiform chromitites of the Bir Tuluwah ophiolite, Saudi Arabia, during Neoproterozoic assembly of the Arabian Shield. *Lithos*, 360–361, 105439. <https://doi.org/10.1016/j.lithos.2020.105439>
- Aitchison, J. C., & Buckman, S. (2012). Accordion vs. quantum tectonics: Insights into continental growth processes from the Paleozoic of eastern Gondwana. *Gondwana Research*, 22(2), 674–680. <https://doi.org/10.1016/j.gr.2012.05.013>
- Arif, M., & Jan, M. Q. (2006). Petrotectonic significance of the chemistry of chromite in the ultramafic–mafic complexes of Pakistan. *Journal of Asian Earth Sciences*, 27(5), 628–646. <https://doi.org/10.1016/j.jseaes.2005.06.004>
- Arnold, G. O., & Rubenach, M. J. (1976). Mafic-ultramafic complexes of the Greenvale area, North Queensland: Devonian intrusions or Precambrian metamorphics? *Journal of the Geological Society of Australia*, 23(2), 119–139. <https://doi.org/10.1080/00167617608728929>
- Barnes, S. J. (2000). Chromite in komatiites, II. Modification during greenschist to mid-amphibolite facies metamorphism. *Journal of Petrology*, 41(3), 387–409. <https://doi.org/10.1093/petrology/41.3.387>
- Barnes, S. J., & Roeder, P. L. (2001). The range of spinel compositions in terrestrial mafic and ultramafic rocks. *Journal of Petrology*, 42(12), 2279–2302. <https://doi.org/10.1093/petrology/42.12.2279>
- Belyaev, V., Gornova, M., Gordienko, I., Karimov, A., Medvedev, A. Y., Ivanov, A., Dril, S., Grigoriev, D., & Belozeroval, O. Y. (2021). Late Cambrian calc-alkaline magmatism during transition from subduction to accretion: Insights from geochemistry of lamprophyre, dolerite and gabbro dikes in the Dzhida terrain, Central Asian orogenic belt. *Lithos*, 386–387, 106044. <https://doi.org/10.1016/j.lithos.2021.106044>
- Berly, T. J., Hermann, J., Arculus, R. J., & Lapierre, H. (2006). Supra-subduction zone pyroxenites from San Jorge and Santa Isabel (Solomon Islands). *Journal of Petrology*, 47(8), 1531–1555. <https://doi.org/10.1093/petrology/egl019>
- Betts, P. G., Withnall, I. W., Armit, R., Donchak, P., & Hutton, L. (2012). Ribbon tectonics: Ordovician and Silurian evolution of North Queensland. In *2012 IAGR Annual Convention and 9th International Symposium on Gondwana to Asia* (pp. 78–79).
- Blewett, R. S., & Black, L. P. (1998). Structural and temporal framework of the Coen Region, north Queensland: Implications for major tectonothermal events in east and north Australia. *Australian Journal of Earth Sciences*, 45(4), 597–609. <https://doi.org/10.1080/08120099808728415>
- Boger, S. D., & Hansen, D. (2004). Metamorphic evolution of the Georgetown Inlier, northeast Queensland, Australia; evidence for an accreted Palaeoproterozoic terrane? *Journal of Metamorphic Geology*, 22(6), 511–527. <https://doi.org/10.1111/j.1525-1314.2004.00528.x>
- Boschi, C., Fruh-Green, G. L., Delacour, A., Karson, J. A., & Kelley, D. S. (2006). Mass transfer and fluid flow during detachment faulting and development of an oceanic core complex, Atlantis Massif (MAR 30N). *Geochemistry, Geophysics, Geosystems*, 7(1), N/A–39. <https://doi.org/10.1029/2005GC001074>
- Božović, M., Prelević, D., Romer, R. L., Barth, M., Van Den Bogaard, P., & Boev, BŽo. (2013). The Demir Kapija Ophiolite, Macedonia (FYROM): A snapshot of subduction initiation within a back-arc. *Journal of Petrology*, 54(7), 1427–1453. <https://doi.org/10.1093/petrology/egt017>
- Brown, M. T., Fuck, R. A., & Dantas, E. L. (2020). Isotopic age constraints and geochemical results of disseminated ophiolitic assemblage from Neoproterozoic mélange, central Brazil. *Precambrian Research*, 339, 105581. <https://doi.org/10.1016/j.precamres.2019.105581>
- Buckman, S., Aitchison, J. C., Nutman, A. P., Bennett, V. C., Saktura, W. M., Walsh, J. M., Kachovich, S., & Hidaka, H. (2018). The Spongtag Massif in Ladakh, NW Himalaya: An Early Cretaceous record of spontaneous, intra-oceanic subduction initiation in the Neotethys. *Gondwana Research*, 63, 226–249. <https://doi.org/10.1016/j.gr.2018.07.003>
- Bultitude, R. J., Donchak, P. J. T., Domagala, J., Fordham, B. G., & Champion, D. C. (1990). Geology and tectonics of the Hodgkinson Province, North Queensland. In *Pacific Rim Congress* (pp. 75–81). Australasian Institute of Mining and Metallurgy.
- Bultitude, R. J., Garrad, P. D., Donchak, P. J. T., Domagala, J., Champion, D. C., Rees, I. D., Mackenzie, D. E., Wellman, P., Knutson, J., Fanning, C. M., Fordham, B. G., Grimes, K. G., Oversby, B. S., Rienks, I. P., Stephenson, P. J., Chappell, B. W., Pain, C. F., Wilford, J. R., Rigby, J. F., & Woodbury, M. J. (1997). Chapter 7: Cairns Region. In J. H. C. Bain & J. J. Draper (Eds.), *North Queensland Geology* (pp. 225–326). AGSO Bulletin, 240.
- Butt, C. R. M., & Cluzel, D. (2013). Nickel laterite ore deposits: Weathered serpentinites. *Elements*, 9(2), 123–128. <https://doi.org/10.2113/gselements.9.2.123>
- Cathelineau, M., Quesnel, B., Gautier, P., Boulvais, P., Couteau, C., & Drouillet, M. (2016). Nickel dispersion and enrichment at the bottom of the regolith: formation of melilite target-like ores in rock block joints (Koniambo Ni deposit, New Caledonia). *Mineralium Deposita*, 51(2), 271–282. <https://doi.org/10.1007/s00126-015-0607-y>
- Cawood, P. A., Kroner, A., Collins, W. J., Kusky, T. M., Mooney, W. D., & Windley, B. F. (2009). Accretionary orogens through Earth history. *Geological Society, London, Special Publications*, 318(1), 1–36. <https://doi.org/10.1144/SP318.1>
- Colás, V., González-Jiménez, J. M., Griffin, W. L., Fanlo, I., Gervilla, F., O'Reilly, S. Y., Pearson, N. J., Kerestedjian, T., & Proenza, J. A. (2014). Fingerprints of metamorphism in chromite: New insights from

- minor and trace elements. *Chemical Geology*, 389, 137–152. <https://doi.org/10.1016/j.chemgeo.2014.10.001>
- Collins, W. J. (2002). Nature of extensional accretionary orogens. *Tectonics*, 21(4), 6–12. <https://doi.org/10.1029/2000TC001272>
- Davis, B. K., Bell, C. C., Lindsay, M., & Henderson, R. A. (2002). A single late orogenic Permian episode of gold mineralization in the Hodgkinson Province, North Queensland, Australia. *Economic Geology*, 97(2), 311–323. <https://doi.org/10.2113/gsecongeo.97.2.311>
- De Keyser, F. (1965). The Barnard metamorphics and their relation to the Barron river metamorphics and the Hodgkinson formation, North Queensland. *Journal of the Geological Society of Australia*, 12(1), 91–103. <https://doi.org/10.1080/00167616508728587>
- Deschamps, F., Godard, M., Guillot, S., & Hattori, K. (2013). Geochemistry of subduction zone serpentinites: A review. *Lithos*, 178, 96–127. <https://doi.org/10.1016/j.lithos.2013.05.019>
- Dick, H. J. B., & Bullen, T. (1984). Chromian spinel as a petrogenetic indicator in abyssal and alpine-type peridotites and spatially associated lavas. *Contributions to Mineralogy and Petrology*, 86(1), 54–76. <https://doi.org/10.1007/BF00373711>
- Dilek, Y., & Furnes, H. (2011). Ophiolite genesis and global tectonics: Geochemical and tectonic fingerprinting of ancient oceanic lithosphere. *Geological Society of America Bulletin*, 123(3–4), 387–411. <https://doi.org/10.1130/B30446.1>
- Dilek, Y., & Furnes, H. (2014). Ophiolites and their origins. *Elements*, 10(2), 93–100. <https://doi.org/10.2113/gselements.10.2.93>
- Dirks, H. N., Sanislav, I. V., & Abu Sharib, A. S. A. (2021). Continuous convergence along the paleo-Pacific margin of Australia during the early Paleozoic: Insights from the Running River Metamorphics, NE Queensland. *Lithos*, 398–399, 106343. <https://doi.org/10.1016/j.lithos.2021.106343>
- Draut, A. E., & Clift, P. D. (2013). Differential preservation in the geologic record of intraoceanic arc sedimentary and tectonic processes. *Earth-Science Reviews*, 116, 57–84. <https://doi.org/10.1016/j.earscirev.2012.11.003>
- Edgar, A., Sanislav, I. V., Dirks, P. H. G. M., & Spandler, C. (2022). Metamorphic diamond from the northeastern margin of Gondwana – paradigm shifting implications for one of Earth's largest orogens. *Science Advances* (in press).
- Elias, M. (2002). Nickel laterite deposits – geological overview, resources and exploitation. In D. R. Cooke & J. Pongratz (Eds.), *Giant ore deposits: Characteristics, genesis and exploration* (pp. 205–220). CODES Special Publication 4, Centre for Ore Deposit Research, University of Tasmania.
- Farrokhpay, S., Cathelineau, M., Blancher, S., Laugier, O., & Filippov, L. (2019). Characterization of Weda Bay nickel laterite ore from Indonesia. *Journal of Geochemical Exploration*, 196, 270–291. <https://doi.org/10.1016/j.gexplo.2018.11.002>
- Fergusson, C. L., Henderson, R. A., Withnall, I. W., Fanning, C. M., Phillips, D., & Lewthwaite, K. J. (2007). Structural, metamorphic, and geochronological constraints on alternating compression and extension in the early Paleozoic Gondwanan Pacific margin, northeastern Australia. *Tectonics*, 26(3), N/A–N/A. <https://doi.org/10.1029/2006TC001979>
- Furnes, H., & Dilek, Y. (2017). Geochemical characterization and petrogenesis of intermediate to silicic rocks in ophiolites: A global synthesis. *Earth-Science Reviews*, 166, 1–37. <https://doi.org/10.1016/j.earscirev.2017.01.001>
- Gamal El Dien, H., Arai, S., Doucet, L.-S., Li, Z.-X., Kil, Y., Fougereuse, D., Reddy, S. M., Saxey, D. W., & Hamdy, M. (2019). Cr-spinel records metasomatism not petrogenesis of mantle rocks. *Nature Communications*, 10(1), 1–12. <https://doi.org/10.1038/s41467-019-13117-1>
- Garrad, P. D., & Bultitude, R. J. (1999). *Geology, mining history and mineralisation of the Hodgkinson and Kennedy Provinces, Cairns region, North Queensland*. Queensland Minerals and Energy Review Series, Queensland Department of Mines and Energy.
- Gleeson, S., Butt, C. R. M., & Elias, M. (2003). Nickel laterites: A review. *SEG Discovery*, 54(54), 1–18. <https://doi.org/10.5382/SEGnews.2003-54.fea>
- Glen, R. A. (2005). The Tasmanides of eastern Australia. *Geological Society, London, Special Publications*, 246(1), 23–96. <https://doi.org/10.1144/GSL.SP.2005.246.01.02>
- Glen, R. A. (2013). Refining accretionary orogen models for the Tasmanides of eastern Australia. *Australian Journal of Earth Sciences*, 60(3), 315–370. <https://doi.org/10.1080/08120099.2013.772537>
- Gray, D., & Foster, D. (2004). Tectonic evolution of the Lachlan Orogen, southeast Australia: historical review, data synthesis and modern perspectives. *Australian Journal of Earth Sciences*, 51(6), 773–817. <https://doi.org/10.1111/j.1400-0952.2004.01092.x>
- Henderson, R. A. (1980). Structural outline and summary geological history for north-eastern Australia. In R. A. Henderson & P. J. Stephenson (Eds.), *The geology and geophysics of North-eastern Australia* (pp. 1–26). Geological Society of Australia.
- Henderson, R. A. (1987). An oblique subduction and transform faulting model for the evolution of the Broken River Province, northern Tasman Orogenic Zone. *Australian Journal of Earth Sciences*, 34(2), 237–249. <https://doi.org/10.1080/08120098708729407>
- Henderson, R. A., & Fergusson, C. L. (2019). Growth and provenance of a Paleozoic subduction complex in the Broken River Province, Mossman Orogen: Evidence from detrital zircon ages. *Australian Journal of Earth Sciences*, 66(5), 607–624. <https://doi.org/10.1080/08120099.2019.1572033>
- Henderson, R. A., Fergusson, C. L., & Withnall, I. W. (2020). Coeval basin formation, plutonism and metamorphism in the Northern Tasmanides: Extensional Cambro-Ordovician tectonism of the Charters Towers Province. *Australian Journal of Earth Sciences*, 67(5), 663–680. <https://doi.org/10.1080/08120099.2020.1747539>
- Henderson, R. A., Innes, B. M., Fergusson, C. L., Crawford, A. J., & Withnall, I. W. (2011). Collisional accretion of a Late Ordovician oceanic island arc, northern Tasman Orogenic Zone, Australia. *Australian Journal of Earth Sciences*, 58(1), 1–19. <https://doi.org/10.1080/08120099.2010.535564>
- Henderson, R., Donchak, P., Withnall, I., Adams, C., Bultitude, R., Champion, D., Davis, B., Hutton, L., & Wormald, R. (2013). Mossman Orogen. In P. A. Jell (Ed.), *Geology of Queensland* (pp. 225–304). Queensland Government.
- Herzberg, C., Vidito, C., & Starkey, N. A. (2016). Nickel-cobalt contents of olivine record origins of mantle peridotite and related rocks. *American Mineralogist*, 101(9), 1952–1966. <https://doi.org/10.2138/am-2016-5538>
- Hole, M., Saunders, A., Marriner, G., & Tarney, J. (1984). Subduction of pelagic sediments: Implications for the origin of Ce-anomalous basalts from the Mariana Islands. *Journal of the Geological Society of London*, 141(3), 453–472. <https://doi.org/10.1144/gsjgs.141.3.0453>
- Irvine, T. (1965). Chromian spinel as a petrogenetic indicator: Part 1. Theory. *Canadian Journal of Earth Sciences*, 2(6), 648–672. <https://doi.org/10.1139/e65-046>
- Irvine, T. (1967). Chromian spinel as a petrogenetic indicator: Part 2. Petrologic applications. *Canadian Journal of Earth Sciences*, 4(1), 71–103. <https://doi.org/10.1139/e67-004>
- Ishwar-Kumar, C., Rajesh, V. J., Windley, B. F., Razakamanana, T., Itaya, T., Babu, E. V. S. S. K., & Sajeev, K. (2018). Chromite chemistry as an indicator of petrogenesis and tectonic setting of the Ranomena ultramafic complex in north-eastern Madagascar. *Geological Magazine*, 155(1), 109–118. <https://doi.org/10.1017/S0016756816000972>
- Jiménez, J. G., Kerestedjian, T., Fernández, J. P., & Linares, F. G. (2009). Metamorphism on chromite ores from the Dobromirski ultramafic massif, Rhodope Mountains (SE Bulgaria). *Geologica Acta*, 7(4), 413–429. <https://revistes.ub.edu/index.php/GEOACTA/article/view/104.000001447>
- Kamenetsky, V., Crawford, A. J., & Meffre, S. (2001). Factors controlling chemistry of magmatic spinel: An empirical study of associated olivine, Cr-spinel and melt inclusions from primitive rocks. *Journal of Petrology*, 42(4), 655–671. <https://doi.org/10.1093/petrology/42.4.655>

- King, R. L., Kohn, M. J., & Eiler, J. M. (2003). Constraints on the petrologic structure of the subduction zone slab-mantle interface from Franciscan Complex exotic ultramafic blocks. *Geological Society of America Bulletin*, 115(9), 1097–1109. <https://doi.org/10.1130/B25255.1>
- Lago, B. L., Rabinowicz, M., & Nicolas, A. (1982). Podiform chromite ore bodies: A genetic model. *Journal of Petrology*, 23(1), 103–125. <https://doi.org/10.1093/petrology/23.1.103>
- Langbein, C. (2010). *The Tectonics and Geochronology of the Mission Beach Granite Complex and Comparisons with the Barnard Metamorphics at Ettu Bay* [Unpublished B Sc(Hons) thesis]. James Cook University.
- Lewis, J. F., Draper, G., Proenza, J. A., Espaillet, J., & Jimenez, J. (2006). Ophiolite-related ultramafic rocks (serpentinities) in the Caribbean Region: A review of their occurrence, composition, origin, emplacement and Ni-laterite soil formation. *Geologica Acta*, 4, 237–263. <https://revistes.ub.edu/index.php/GEOACTA/article/view/105.000000368>
- Maier, W. D., Barnes, S. J., Bandyayera, D., Livesey, T., Li, C., & Ripley, E. (2008). Early Kibaran rift-related mafic-ultramafic magmatism in western Tanzania and Burundi: Petrogenesis and ore potential of the Kapalagulu and Musongati layered intrusions. *Lithos*, 101(1–2), 24–53. <https://doi.org/10.1016/j.lithos.2007.07.015>
- Manton, R. J., Buckman, S., Nutman, A. P., & Bennett, V. C. (2017). Exotic island arc Paleozoic terranes on the eastern margin of Gondwana: Geochemical whole rock and zircon U–Pb–Hf isotope evidence from Barry Station, New South Wales, Australia. *Lithos*, 286–287, 125–150. <https://doi.org/10.1016/j.lithos.2017.06.002>
- Middlemost, E. A. K. (1994). Naming materials in the magma/igneous rock system. *Earth-Science Reviews*, 37(3–4), 215–224. [https://doi.org/10.1016/0012-8252\(94\)90029-9](https://doi.org/10.1016/0012-8252(94)90029-9)
- Miyashiro, A. (1974). Volcanic rock series in island arcs and active continental margins. *American Journal of Science*, 274(4), 321–355. <https://doi.org/10.2475/ajs.274.4.321>
- Miyashiro, A., & Shido, F. (1975). Tholeiitic and calc-alkaline series in relation to the behaviors of titanium, vanadium, chromium, and nickel. *American Journal of Science*, 275(3), 265–277. <https://doi.org/10.2475/ajs.275.3.265>
- Müntener, O., Kelemen, P. B., & Grove, T. L. (2001). The role of H₂O during crystallization of primitive arc magmas under uppermost mantle conditions and genesis of igneous pyroxenites: An experimental study. *Contributions to Mineralogy and Petrology*, 141(6), 643–658. <https://doi.org/10.1007/s004100100266>
- Murgulov, V., Beyer, E., Griffin, W. L., O'Reilly, S. Y., Walters, S. G., & Stephens, D. (2007). Crustal evolution in the Georgetown Inlier, North Queensland, Australia: A detrital zircon grain study. *Chemical Geology*, 245(3–4), 198–218. <https://doi.org/10.1016/j.chemgeo.2007.08.001>
- O'Neill, H. S. C., & Palme, H. (2014). Cosmochemical estimates of mantle composition. In R. W. Carlson (Ed.), *Treatise on geochemistry* (pp. 1–39). Elsevier. <https://doi.org/10.1016/B0-08-043751-6/02177-0>
- Pearce, J. (2014). Immobile element fingerprinting of ophiolites. *Elements*, 10(2), 101–108. <https://doi.org/10.2113/gselements.10.2.101>
- Pearce, J. A., & Cann, J. R. (1973). Tectonic setting of basic volcanic rocks determined using trace element analyses. *Earth and Planetary Science Letters*, 19(2), 290–300. [https://doi.org/10.1016/0012-821X\(73\)90129-5](https://doi.org/10.1016/0012-821X(73)90129-5)
- Pearce, J. A., Alabaster, T., Shelton, A. W., & Spearle, M. P. (1981). The Oman ophiolite as a Cretaceous arc-basin complex: Evidence and implications. *Philosophical Transactions of the Royal Society of London*, 300, 299–317. <https://doi.org/10.2113/gselements.10.2.101>
- Poblete, J. A., Dirks, P. H. G. M., Chang, Z., Huizenga, J. M., Griessmann, M., & Hall, C. (2021). The Watershed Tungsten Deposit, northeast Queensland, Australia: Permian metamorphic tungsten mineralization overprinting Carboniferous magmatic tungsten. *Economic Geology*, 116(2), 427–451. <https://doi.org/10.5382/econgeo.4791>
- Proenza, J. A., Zaccarini, F., Escayola, M., Cábana, C., Schalamuk, A., & Garuti, G. (2008). Composition and textures of chromite and platinum-group minerals in chromitites of the western ophiolitic belt from Pampean Ranges of Córdoba, Argentina. *Ore Geology Reviews*, 33(1), 32–48. <https://doi.org/10.1016/j.oregeorev.2006.05.009>
- Rinne, M., & Hollings, P. (2013). The characteristics and origin of the Big Lake mafic-ultramafic-hosted volcanogenic massive sulfide occurrence, Marathon, Ontario, Canada. *Economic Geology*, 108(4), 719–738. <https://doi.org/10.2113/econgeo.108.4.719>
- Rollinson, H. (2005). Chromite in the mantle section of the Oman ophiolite: A new genetic model. *The Island Arc*, 14(4), 542–550. <https://doi.org/10.1111/j.1440-1738.2005.00482.x>
- Rollinson, H., & Adetunji, J. (2013). Mantle podiform chromitites do not form beneath mid-ocean ridges: A case study from the Moho transition zone of the Oman ophiolite. *Lithos*, 177, 314–327. <https://doi.org/10.1016/j.lithos.2013.07.004>
- Rosenbaum, G. (2018). The Tasmanides: Phanerozoic tectonic evolution of eastern Australia. *Annual Review of Earth and Planetary Sciences*, 46(1), 291–325. <https://doi.org/10.1146/annurev-earth-082517-010146>
- Schroeder, T., & John, B. E. (2004). Strain localization on an oceanic detachment fault system, Atlantis Massif, 30°N, Mid-Atlantic Ridge. *Geochemistry, Geophysics, Geosystems*, 5(11), N/A–30. <https://doi.org/10.1029/2004GC000728>
- Shervais, J. W. (1982). Ti–V plots and the petrogenesis of modern and ophiolitic lavas. *Earth and Planetary Science Letters*, 59(1), 101–118. [https://doi.org/10.1016/0012-821X\(82\)90120-0](https://doi.org/10.1016/0012-821X(82)90120-0)
- Shervais, J. W. (2001). Birth, death, and resurrection: The life cycle of suprasubduction zone ophiolites. *Geochemistry, Geophysics, Geosystems*, 2(1), N/A–N/A. <https://doi.org/10.1029/2000GC000080>
- Shi, R., Griffin, W. L., O'Reilly, S. Y., Huang, Q., Zhang, X., Liu, D., Zhi, X., Xia, Q., & Ding, L. (2012). Melt/mantle mixing produces podiform chromite deposits in ophiolites: Implications of Re–Os systematics in the Dongqiao Neo-Tethyan ophiolite, northern Tibet. *Gondwana Research*, 21(1), 194–206. <https://doi.org/10.1016/j.gr.2011.05.011>
- Spandler, C., Hermann, J., Faure, K., Mavrogenes, J., & Arculus, R. (2008). The importance of talc and chlorite “hybrid” rocks for volatile recycling through subduction zones; evidence from the high-pressure subduction melange of New Caledonia. *Contributions to Mineralogy and Petrology*, 155(2), 181–198. <https://doi.org/10.1007/s00410-007-0236-2>
- Takla, M. A., Trommsdorff, V., Basta, F. F., & Surour, A. A. (2004). Margarite in ultramafic alteration zones (Blackwall) A new occurrence in Barramiya Area. *European Journal of Mineralogy*, 15(6), 991–999. <https://doi.org/10.1127/0935-1221/2003/0015-0991>
- Vos, I. M. A., Bierlein, F. P., & Teale, G. S. (2005). Genesis of orogenic-gold deposits in the Broken River Province, northeast Queensland. *Australian Journal of Earth Sciences*, 52(6), 941–958. <https://doi.org/10.1080/08120090500375190>
- Vos, I. M. A., Bierlein, F. P., Barlow, M. A., & Betts, P. G. (2006). Resolving the nature and geometry of major fault systems from geophysical and structural analysis: The Palmerville Fault in NE Queensland, Australia. *Journal of Structural Geology*, 28(11), 2097–2108. <https://doi.org/10.1016/j.jsg.2006.07.016>
- Wang, C. Y., Zhou, M-F., & Zhao, D. (2005). Mineral chemistry of chromite from the Permian Jinbaoshan Pt–Pd–sulphide-bearing ultramafic intrusion in SW China with petrogenetic implications. *Lithos*, 83(1–2), 47–66. <https://doi.org/10.1016/j.lithos.2005.01.003>
- Wang, Z., Li, M. Y. H., Liu, Z. –R. R., & Zhou, M-F. (2021). Scandium: Ore deposits, the pivotal role of magmatic enrichment and future exploration. *Ore Geology Reviews*, 128, 103906. <https://doi.org/10.1016/j.oregeorev.2020.103906>
- Wang, Z., Sun, S., Li, J., & Hou, Q. (2002). Petrogenesis of tholeiite associations in Kudi ophiolite (western Kunlun Mountains, northwestern China): Implications for the evolution of back-arc basins. *Contributions to Mineralogy and Petrology*, 143(4), 471–483. <https://doi.org/10.1007/s00410-002-0358-5>
- Williams-Jones, A. E., & Vasyukova, O. (2018). The economic geology of scandium, the runt of the rare earth element litter. *Economic Geology*, 113(4), 973–988. <https://doi.org/10.5382/econgeo.2018.4579>
- Winchester, J. A., & Floyd, P. A. (1977). Geochemical discrimination of different magma series and their differentiation products using

- immobile elements. *Chemical Geology*, 20, 325–343. [https://doi.org/10.1016/0009-2541\(77\)90057-2](https://doi.org/10.1016/0009-2541(77)90057-2)
- Withnall, I. W., & Cranfield, L. C. (2013). Geological framework. In P. Jell (Ed.), *The geology of Queensland* (pp. 13–34). Queensland Government.
- Withnall, I. W., & Henderson, R. A. (2012). Accretion on the long-lived continental margin of northeastern Australia. *Episodes*, 35(1), 166–176. <https://doi.org/10.18814/epiiugs/2012/v35i1/016>
- Xiong, F., Yang, J., Robinson, P. T., Xu, X., Liu, Z., Li, Y., Li, J., & Chen, S. (2015). Origin of podiform chromitite, a new model based on the Luobusa ophiolite, Tibet. *Gondwana Research*, 27(2), 525–542. <https://doi.org/10.1016/j.gr.2014.04.008>
- Yellappa, T., Chetty, T. R. K., Tsunogae, T., & Santosh, M. (2010). The Manamedu Complex: Geochemical constraints on Neoproterozoic suprasubduction zone ophiolite formation within the Gondwana suture in southern India. *Journal of Geodynamics*, 50(3–4), 268–285. <https://doi.org/10.1016/j.jog.2009.12.004>
- Yilmaz, A., & Yilmaz, H. (2013). Ophiolites and ophiolitic mélanges of Turkey: A review. *Geological Bulletin of Turkey*, 56, 61–114. <https://doi.org/10.1007/s12583-016-0679-3>
- Yu, H., Zhang, H. F., Zou, H. B., & Yang, Y. H. (2019). Minor and trace element variations in chromite from the Songshugou dunites, North Qinling Orogen: Evidence for amphibolite-facies metamorphism. *Lithos*, 328–329, 146–158. <https://doi.org/10.1016/j.lithos.2019.01.009>
- Zaccarini, F., Garuti, G., Proenza, J. A., Campos, L., Thalhammer, O. A., Aiglsperger, T., & Lewis, J. F. (2011). Chromite and platinum group elements mineralization in the Santa Elena Ultramafic Nappe (Costa Rica): Geodynamic implications. *Geologica Acta*, 9(3–4), 407–423. <https://revistes.ub.edu/index.php/GEOACTA/article/view/105.000001696>
- Zeissink, H. (1969). The mineralogy and geochemistry of a nickeliferous laterite profile (Greenvale, Queensland, Australia). *Mineralium Deposita*, 4(2), 132–152. <https://doi.org/10.1007/BF00208049>
- Zheng, Y. F., Chen, R. X., Xu, Z., & Zhang, S. B. (2016). The transport of water in subduction zones. *Science China Earth Sciences*, 59(4), 651–682. <https://doi.org/10.1007/s11430-015-5258-4>
- Zhou, M-F., & Robinson, P. T. (1997). Origin and tectonic environment of podiform chromite deposits. *Economic Geology*, 92(2), 259–262. <https://doi.org/10.2113/gsecongeo.92.2.259>
- Zucchetto, R. G., Henderson, R. A., Davis, B. K., & Wysoczanski, R. (1999). Age constraints on deformation of the eastern Hodgkinson Province, north Queensland: New perspectives on the evolution of the northern Tasman Orogenic Zone. *Australian Journal of Earth Sciences*, 46(1), 105–114. <https://doi.org/10.1046/j.1440-0952.1999.00689.x>